

# Block model for the XY-type Landau-Ginzburg-Wilson Hamiltonian with an inhomogeneous temperature

X.T. Wu

*Department of Physics, Beijing Normal University, Beijing, 100875, China*

(Dated: January 23, 2012)

The phase fluctuation near the saddle point solution of the XY-type Landau-Ginzburg-Wilson Hamiltonian with random temperature is studied. For the modes with lowest eigenvalue, the systems is self-organized into blocks, which are coupled as a XY model with random bond. The couplings obtained in this way agree with those by domain wall method.

PACS numbers: 05.70.-a, 05.70.Fh+q, 64.60.-i, 64.60.Bd

## I. INTRODUCTION

In recent years more and more experiments show locally ordered regions (LOR). Localized Bose-Einstein condensation above the global superfluid transition temperature is revealed in superfluid transition of  $^4\text{He}$  in silica gel [1, 2]. It is well-known that for some granular superconductors, on the insulating side of the superconductor insulator transition, each grain is separately and independently superconducting while a transport measurement shows the film to be insulating [3]. In recent experiment on amorphous NbN films, pseudo-gapped state due to the locally superconducting islands is discovered [4]. The nucleation of pairing gaps in nanoscale regions above  $T_c$  is also found in the high- $T_c$  superconductor  $\text{Bi}_2\text{Sr}_2\text{CaCu}_2\text{O}_{8+\delta}$  [5]. In addition, a local metallic state is observed in globally insulating  $\text{La}_{1.24}\text{Sr}_{1.76}\text{Mn}_2\text{O}_7$  well above the metal-insulator transition [6]. The existence of Ferromagnetic region in the paraphase of  $\text{La}_{1-x}\text{Ba}_x\text{MnO}_3$  is discovered [7].

To understand the relation between LOR and the phase transition in a general way, the saddle point equation of Landau-Ginzburg Hamiltonian with random temperature is solved recently [8, 9]. LOR is explicitly shown in these solutions. Moreover it is found that there exist many excited solutions, which minimize the Hamiltonian locally in the configuration space. These solutions can be described by the block model (in the following we call it B model), in which the system is self-organized into blocks. These blocks behave like superspins and are coupled with their neighbors. In reference [10], a general method to calculate the couplings between adjoined blocks is proposed. This method is based on the free energy increasing of domain wall (DW) between the adjoined blocks. So we call this method DW method.

However for the systems with continuous order parameter, such as superfluid, superconductor, the continuous phase fluctuation about the saddle point solution should be taken into account. In DW method this kind of fluctuation is absent. In this paper we study the XY-type Landau-Ginzburg-Wilson (LGW) Hamiltonian with random temperature. We propose a Gaussian approximation to study the continuous phase fluctuation near the saddle point solutions. We will show that

(1). The system is still be organized into blocks given by the DW method.

(2). For the modes with lower eigenvalues, the couplings between the blocks are XY-type like a Josephson junction array and the couplings are approximately equal to those given by the DW method. The blocks are coupled like XY-type spins.

Our paper is arranged as follows. In section II, the model of XY-type Landau-Ginzburg-Wilson (LGW) Hamiltonian with random temperature is given. In section III, one dimensional case is discussed. In section IV, two dimensional case is discussed. Section V is a summary.

## II. THE MODEL

We consider the XY-type Landau-Ginzburg-Wilson (LGW) Hamiltonian with random temperature

$$H = \int d\mathbf{r} \left\{ \frac{1}{2} |\nabla \phi(\mathbf{r})|^2 + \frac{1}{2} t(\mathbf{r}) \phi^2(\mathbf{r}) + \frac{1}{4} \phi^4(\mathbf{r}) \right\}, \quad (1)$$

where

$$\phi = (\phi_x, \phi_y), \quad \phi^2 = \phi_x^2 + \phi_y^2, \quad |\nabla \phi|^2 = |\nabla \phi_x|^2 + |\nabla \phi_y|^2, \quad (2)$$

and  $t(\mathbf{r}) = t + \tilde{t}(\mathbf{r})$ , and  $t, \tilde{t}(\mathbf{r})$  are the average reduced temperature and the random part caused by the disorder respectively. The parameters are scaled according to the references [8, 10].

The saddle point equations are given by

$$-\nabla^2 \phi_x(\mathbf{r}) + [t(\mathbf{r}) + \phi^2(\mathbf{r})] \phi_x(\mathbf{r}) = 0, \quad (3)$$

$$-\nabla^2 \phi_y(\mathbf{r}) + [t(\mathbf{r}) + \phi^2(\mathbf{r})] \phi_y(\mathbf{r}) = 0. \quad (4)$$

Through this paper we assume the saddle point solutions are along  $\phi_x$  direction,

$$\phi_x = \phi_x^{(\nu)}, \quad \phi_y = 0. \quad (5)$$

where  $\nu$  is used to label the excited states.

Substituting the saddle point solution into Eq. (1), one get the free energy [11]

$$F_\nu = H(\{\phi_x^{(\nu)}\}) = - \int d\mathbf{r} \frac{1}{4} (\phi_x^{(\nu)})^4(\mathbf{r}), \quad (6)$$

for the  $\nu$ th solution.

If we assume the solution is along  $\phi_x$  direction and ignore the fluctuation in  $\phi_y$  direction, the problem is reduced to be Ising-type. It has been shown that in that case the system is self-organized into blocks and the blocks are coupled like Ising-spins [9]. The couplings between blocks can be obtained by calculating the free energy increase due to the domain wall [10]. If  $(\phi_x, \phi_y)$  is regarded as a complex parameter, letting  $\phi_y = 0$  is a constraint that only the phase of 0 and  $\pi$  is allowed. If we take the fluctuation of  $\phi_y$  into account, the phase fluctuation becomes continuous.

In order to write the Hamiltonian in terms of the amplitude and phase of the order parameter, we introduce

$$\phi_x = \Phi \cos \theta, \quad \phi_y = \Phi \sin \theta. \quad (7)$$

Then LGW Hamiltonian becomes

$$H = \int d\mathbf{r} \left\{ \frac{1}{2} [|\nabla \Phi|^2 + \Phi^2 |\nabla \theta|^2] + \frac{1}{2} t(\mathbf{r}) \Phi^2 + \frac{1}{4} \Phi^4 \right\}. \quad (8)$$

In this form, we can see that the free energy increase induced by the variation of phase is proportioned to the square of amplitude.

### III. ONE-DIMENSIONAL CASE

#### A. The method of domain wall

As an example, we first consider a system with size being 14 consisting of 7 wells and 7 barriers, i.e. the temperature field is given by

$$t(\xi) = \begin{cases} t_b; & 2i - 2 < \xi \leq 2i - 1, \\ t_w; & 2i - 1 < \xi \leq 2i. \end{cases} \quad (9)$$

where  $i = 1, 2, \dots, 7$ . Here we let the spatial coordinate be  $\xi$  to distinguish from the directions of order parameter.

Obviously this system is periodic with period of 2. The ground state solution  $\phi_x^{(0)}$  for the temperature field with  $t_w = -30, t_b = 10$  is shown in the Fig. (1a). The saddle point equation is solved by finite-difference method with step  $h = 0.025$  [12]. The saddle point solution is approximately equal to  $\sqrt{-t_w}$  at the centers of wells and decays to very small in the barriers [8]. Using the DW method, we can show that there are 7 elementary blocks and can calculate the couplings between the adjoined blocks. For example, letting the initial value of  $\phi_x$  be negative in the first well and positive at other positions, we will get the excited solutions  $\phi_x^{(1)}$ , which is also shown in the Fig. (1a). The spatial range of the first block is given by  $\phi_x^{(1)}(\xi) < 0$ . Explicitly it is  $0.5 < \xi \leq 2.5$ .

Similarly, letting the initial value of  $\phi_x$  be negative in the second well and positive at other positions, we will get the excited solutions  $\phi_x^{(2)}$ . The spatial range of the second block is  $2.5 < \xi \leq 4.5$ . We do not show it in figure since its shape is the same as  $\phi_x^{(1)}$  and can be

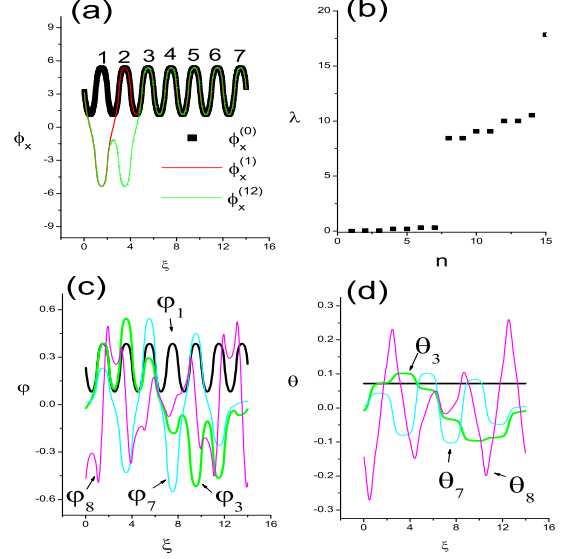


FIG. 1: (Color on line) (a) The ground state and two excited state solutions with temperature field with  $t_w = -30, t_b = 10$ . (b) The first 15 eigenvalues of Eq. (17). (c) 4 typical eigen functions. (d) The phase variations corresponding to the eigenfunctions in (c). The straight line is  $\Theta_1$ .

obtained by shifting  $\phi_x^{(1)}$  in  $\xi$ -axis by 2. Therefore the spatial ranges of the 7 elementary blocks are given by  $2(i-1) + 0.5 < \xi \leq 2i + 0.5$ , where satisfy  $\phi_x^{(i)} < 0$ , for  $i = 1, 2, \dots, 7$ .

Here we give a general method to get the spatial range of the elementary block. For the general disordered cases, the domain wall of elementary block can be obtained by the method of opening windows [10]. The spatial range of this block is that surrounded by the domain wall.

Letting the initial value of  $\phi_x$  be negative in both the first and second well and positive at other positions, we will get the excited solutions  $\phi_x^{(12)}$ . Substituting the solutions  $\phi_x^{(0)}, \phi_x^{(1)}, \phi_x^{(2)}, \phi_x^{(12)}$  into Eq. (6), we get the free energies  $F_0, F_1, F_2, F_{12}$ , and the free energy increases  $f_1 = F_1 - F_0, f_2 = F_2 - F_0$  and  $f_{12} = F_{12} - F_0$ . Then the couplings between blocks is given by [10]

$$K_{12}^{(D)} = (f_1 + f_2 - f_{12})/2. \quad (10)$$

Here we use “(D)” to denote the DW method. In this way we get the couplings between adjoined blocks. Then the free energy of  $\nu$ th state is given by

$$f_\nu = - \sum_i K_{i,i+1} (\sigma_i \sigma_{i+1} - 1)/2 \quad (11)$$

where  $\sigma_i$  is the sign of the  $i$ th block in the  $\nu$ th solution.

The couplings between adjoined blocks with  $t_w = -30$  at different  $t_b$  are given in table 1.

### B. Gauss approximation: expansion around the ground state

Considering the symmetry of the system, the effective Hamiltonian should be XY type rather than Ising type. Simply let  $\sigma_i, \sigma_j$  be unit two dimensional vectors, i.e.

$$\sigma = (\sigma_x, \sigma_y), \quad \sigma_x^2 + \sigma_y^2 = 1 \quad (12)$$

Eq. (11) becomes a XY model. DW method does not contradict to this conclusion and it only provided us the excited states with  $\sigma_x = \pm 1, \sigma_y = 0$ .

To study the cases with continuous  $\sigma$ , we expand the GLW Hamiltonian near the ground state saddle point solution. Let

$$\tilde{\phi}_x = \phi_x - \phi_x^{(0)}, \quad \tilde{\phi}_y = \phi_y - \phi_y^{(0)} = \phi_y, \quad (13)$$

and we consider the Gauss approximation that

$$H \approx F_0 + \delta H_x + \delta H_y \quad (14)$$

where  $F_0$  is the free energy of ground state solution and

$$\delta H_x = \int_0^{14} \frac{1}{2} \left[ \left( \frac{d\tilde{\phi}_x}{d\xi} \right)^2 + [t + 3(\phi_x^{(0)})^2] \tilde{\phi}_x^2 \right] d\xi \quad (15)$$

$$\delta H_y = \int_0^{14} \frac{1}{2} \left[ \left( \frac{d\tilde{\phi}_y}{d\xi} \right)^2 + [t + (\phi_x^{(0)})^2] \tilde{\phi}_y^2 \right] d\xi, \quad (16)$$

where the quartic terms are omitted.

Because the saddle point solution is assumed along  $\phi_x$  direction, the fluctuation of  $\phi_x$  is the amplitude fluctuation and that of  $\phi_y$  is just the phase fluctuation. The eigenmodes of  $\tilde{\phi}_y$  satisfies the following equation

$$-\frac{d^2 \varphi}{d\xi^2} + [t + (\phi_x^{(0)})^2] \varphi_n = \lambda_n \varphi_n \quad (17)$$

where  $\lambda_n$  is eigenvalues and  $\varphi_n$  are the eigenfunctions. Then we have

$$\delta H_y = \frac{1}{2} \sum_n \lambda_n a_n^2 \quad (18)$$

where

$$a_n = \int_0^{14} \tilde{\phi}_y \varphi_n d\xi. \quad (19)$$

The contribution of phase fluctuation to the partition function is given by

$$z_y = \int D\tilde{\phi}_y e^{-\delta H_y} = \int \prod_n da_n e^{-\frac{1}{2} \sum_n \lambda_n a_n^2} \quad (20)$$

We discretize the equation (17) with grid of step 0.025 and solve it by LAPACK, which is a package to deal matrix. The first 15 eigenvalues are shown in Fig. 1(b) and some eigenfunctions are shown in Fig. 1(c).

The modes of  $\tilde{\phi}_y$  with lower eigenvalues give the main contribution beyond the saddle point solution. As shown in Fig. (1b), where  $t_i = -30, t_b = 10$ , the first 7 eigenvalues are remarkably lower than other eigenvalues. Then they possess much bigger thermodynamic amplitudes than other modes according to Eq. (20).

In order to understand the first 7 eigenfunctions more clearly, we introduce

$$\tan \Theta_n = \varphi_n / \phi_x^{(0)} \quad (21)$$

and show  $\Theta_1, \Theta_3, \Theta_7, \Theta_8$  in Fig. (1d). This function show the phase variation of the eigenfunctions. As one can see in Fig. (1d),  $\Theta_1$  is a constant. This is because that the first eigenfunction  $\varphi_1$  has eigenvalue  $\lambda_1 = 0$  and satisfies

$$\varphi_1 = \phi_x^{(0)} / \int_0^{14} d\xi (\phi_x^{(0)})^2. \quad (22)$$

This can be shown by comparing the equation (3) and (17). This eigenfunction corresponds to a global rotation, so its eigenvalue is zero.  $\lambda_1 = 0$  corresponds to the infrared divergence.

Observing  $\Theta_3, \Theta_7$ , one can see that the variation of phase in the wells are obviously smaller than in barriers.  $\Theta_2, \Theta_4, \Theta_5, \Theta_6$  also have the this feature. From Eq.(8), we can see that the free energy increase related to the phase fluctuation is proportional to the square of ground state saddle point solution. In the barriers, the saddle point solution is much smaller than in the wells. Therefore phase fluctuation in the barriers induced small energy increase. The eighth eigenfunction does not have such a feature and its energy is remarkably higher than the first 7 modes. This means that for the first 7 modes, each block can be regarded as a unit. The phase variation inside the block can be ignored and only the phase difference between blocks are concerned. Therefore we introduce the block functions

$$\Psi_i(\xi) = \begin{cases} \phi_x^{(0)}(\xi); & \phi_x^{(i)} < 0, \\ 0; & \text{other cases.} \end{cases} \quad (23)$$

where the spatial range given by  $\phi_x^{(i)} < 0$  is explicitly given by  $2(i-1) + 0.5 < \xi < 2i + 0.5$  as mentioned in subsection III A.

Then we assume that

$$\tilde{\phi}_y \approx \sum_{i=1}^7 \theta_i \Psi_i, \quad (24)$$

where only one phase is assigned to each block, then Eq. (18) becomes

$$\delta H_y = \sum_{i=1}^7 \sum_{j=1}^7 J_{ij} \theta_i \theta_j \quad (25)$$

where

$$J_{ij} = \frac{1}{2} \sum_{n=1}^7 \lambda_n A_{i,n} A_{j,n} \quad (26)$$

with

$$A_{i,n} = \int_0^{14} \Psi_i(\xi) \varphi_n(\xi) d\xi. \quad (27)$$

In this effective Hamiltonian, we only take the first 7 modes into account.

On one hand the effective Hamiltonian Eq. (28) can be given by the expansion of the following XY model approximately

$$\delta H_y \approx - \sum_{i < j} K_{ij}^{(G)} (\cos(\theta_i - \theta_j) - 1)/2 \quad (28)$$

for  $\theta_i, \theta_j \ll 1$  with

$$\begin{aligned} J_{ii} &= (K_{i,i-1}^{(G)} + K_{i,i+1}^{(G)})/4, \\ J_{i,i+1} &= J_{i+1,i} = -K_{i,i+1}^{(G)}/4, \\ J_{i,i+2} &= J_{i+2,i} = -K_{i,i+2}^{(G)}/4 \end{aligned} \quad (29)$$

where “(G)” is used to denote the method of Gauss approximation. This Hamiltonian is consistent with Eq. (11) obtained by DW method. If we regard Eq. (11) is a special form of Eq. (28) with  $\theta_i = 0, \pi$ , it should have  $K_{i,i+1}^{(D)} = K_{i,i+1}^{(G)}$ . We investigate the cases with different  $t_b$  with fixed  $t_w = -30$ . The numerical results for matrix elements of  $J_{ij}$  and the couplings  $K_{i,i+1}^{(D)}$  by DW method are shown in Table 1. As shown in table 1 and Eq. (29),  $K_{i,i+1}^{(D)} \approx K_{i,i+1}^{(G)}$  is satisfied even for  $t_b = 0$  in an error less than 20%. For higher  $t_b$ , two methods agree with each other very well. At  $t_b = 40.0$ , the relative difference between  $K_{i,i+1}^{(D)}$  and  $K_{i,i+1}^{(G)}$  is less than  $10^{-5}$ . In addition the couplings between next nearest neighbors are much smaller than the that between nearest neighbors, i.e.  $J_{i,i+2} \ll J_{i,i+1}$ . This indicates the approximation of nearest neighbors is good enough.

Moreover Eq. (28) is the well-known Josephson’s junctions Hamiltonian. This result is natural because the wells and barriers given in Eq. (9) is a Josephson junction lattice.

$t_b$	$K_{i,i+1}^{(D)}/4$	$J_{i,i}$	$-J_{i,i+1}$	$J_{i,i+2}$	$R_\phi$	$R_\lambda$
40.0	0.070354	0.13905	0.070357	$8.71 \times 10^{-5}$	25.1	549
30.0	0.16205	0.32199	0.16195	$4.70 \times 10^{-4}$	15.5	229
20.0	0.41458	0.81634	0.41174	$3.10 \times 10^{-3}$	8.91	84.5
10.0	1.2046	2.2608	1.15497	$2.50 \times 10^{-2}$	4.72	26.4
0.0	3.7826	5.8779	3.1027	$1.87 \times 10^{-1}$	2.51	7.95

Table 1: Couplings  $K^{(D)}$  by DW method and  $J_{ij}$  by Gauss approximation at different  $t_b$  and  $t_w = -30.0$ .

We introduce two ratios.  $R_\phi$  is the ratio between the maximum of  $\phi_x^{(0)}$  at the center of well and its minimum at the center of barrier. Another ratio is defined by  $R_\lambda = \lambda_8/\lambda_7$ . At higher  $t_b$ , the saddle point solution in the barriers are very small,  $R_\phi$  is very large, the phase

variation concentrate more in the barriers, so the assumption is good that the phase variation inside the well is ignored. For lower  $t_b$ , the saddle point solution in the barriers is no longer small and the phase variation does not favor concentrating in the barriers. The assumption ignoring the phase variation inside the well is no longer good. Consider the extreme case  $t_b = t_w$ , no block can be well defined. At higher  $t_b$ , the ratio  $R_\phi$  is very large, taking only the first 7 eigenmodes and neglecting other modes is a good approximation. For lower  $t_b$ , the ratio  $R_\phi$  becomes small, the approximation to neglect other modes becomes bad.

This approximation is similar to the phase-only approximation to simplify the Ginzburg-Landau model to XY model [13], in which the modulus of each blocks are fixed and only their phases are allowed to fluctuate.

We summarize the Gauss approximation method as follows:

- (1). Obtaining the saddle point solutions and spatial ranges of blocks by DW method.
- (2). Solving the eigenmodes of  $\tilde{\phi}_y$ .
- (3). Defining the block functions as in Eq. (23) and expanding the Hamiltonian as in Eq. (28), then we can get the couplings.

### C. Gauss approximation: expansion around the excited state

We can also expand the GLW Hamiltonian near the excited states with the above method. Consider the excited state shown in Fig. (2a). The excited state solution is obtained by assign the initial value be negative in the 4th barrier and positive at other sites. Therefore we denote it by  $\phi_x^{(4)}$ . Let

$$\tilde{\phi}_x = \phi_x - \phi_x^{(4)}, \quad \tilde{\phi}_y = \phi_y - \phi_y^{(4)} = \phi_y, \quad (30)$$

and we consider the Gauss approximation that

$$H \approx F_4 + \delta H_x + \delta H_y \quad (31)$$

where  $F_4$  is the free energy of excited state  $\phi_x^{(4)}$  solution and

$$\delta H_x = \int_0^{14} d\xi \frac{1}{2} [(\frac{d\tilde{\phi}_x}{d\xi})^2 + [t + 3(\phi_x^{(4)})^2]\tilde{\phi}_x^2] \quad (32)$$

$$\delta H_y = \int_0^{14} \frac{1}{2} [(\frac{d\tilde{\phi}_y}{d\xi})^2 + [t + (\phi_x^{(4)})^2]\tilde{\phi}_y^2], \quad (33)$$

where the quartic terms are omitted.

The eigenmodes of  $\tilde{\phi}_y$  satisfies the following equation

$$-\frac{d^2 \varphi}{d\xi^2} + [t + (\phi_x^{(4)})^2]\varphi = \lambda_n \varphi \quad (34)$$

where  $\lambda_n$  is eigenvalues and  $\varphi_n$  are the eigenfunctions.

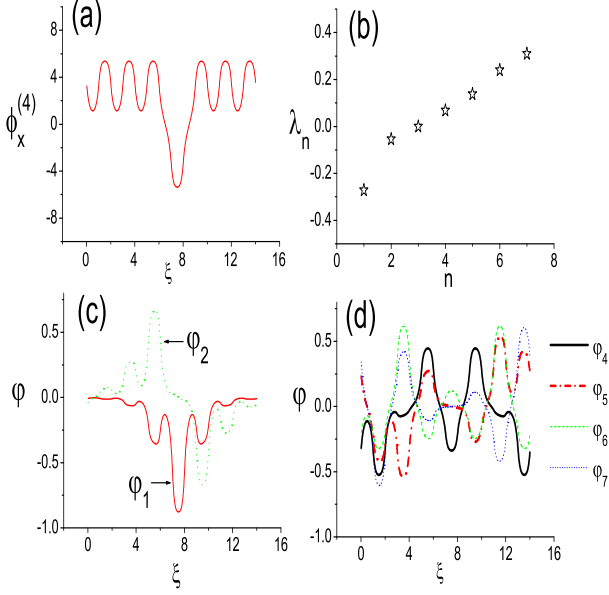


FIG. 2: (Color on line) (a) The excited state solution  $\phi_x^{(4)}$ . (b) The first 7 eigenvalues of Eq. (34). (c) The eigenfunctions  $\phi_1, \phi_2$ . (d) The eigenfunctions  $\phi_4, \phi_5, \phi_6, \phi_7$ .

The first 7 eigenvalues are shown in Fig. 2(b) and some eigenfunctions are shown in Fig. 2(c) and 2(d). The first two eigenvalue are negative. This means that the first two modes can cause the free energy to decrease.

The third eigenfunction  $\phi_3$  has eigenvalue  $\lambda_3 = 0$  and it satisfies that

$$\phi_3 = \phi_x^{(4)} / \int_0^{14} d\xi (\phi_x^{(4)})^2. \quad (35)$$

because  $\phi^{(4)}$  also satisfies the saddle point equation (3) and Eq. (34) with  $\lambda = 0$ . This mode corresponds to a global rotation.

Similarly we introduce the block functions

$$\Psi_i(\xi) = \begin{cases} \phi_x^{(4)}; & 2(i-1) + 0.5 < \xi \leq 2i + 0.5, \\ 0; & \text{other cases.} \end{cases} \quad (36)$$

and assume that

$$\tilde{\phi}_y \approx \sum_{i=1}^7 \theta_i \Psi_i. \quad (37)$$

Here it should be noted that the phase of the 4th block is  $\pi + \theta_4$  rather than  $\theta_4$ .

$t_b$	$K_{i,i+1}^{(D)}/4$	$-J_{7,1}$	$-J_{1,2}$	$-J_{2,3}$	$J_{3,4}$
40.0	0.070354	0.070357	0.70357	0.070176	0.070510
30.0	0.16205	0.16195	0.16195	0.16097	0.16306
20.0	0.41458	0.41174	0.41174	0.40510	0.42221
10.0	1.2046	1.1549	1.1548	1.0965	1.2866
0.0	3.7826	3.1012	3.0891	2.4233	4.7582

Table 2: Couplings  $K^{(D)}$  by DW method and  $J_{ij}$  by Gauss approximation at different  $t_b$  and  $t_w = -30.0$  for the excited state  $\phi_x^{(4)}$ .

For  $\theta_i \ll 1$ , the effective Hamiltonian of the fluctuation about this excited state can be expanded into following XY model approximately

$$\delta H_y \approx - \sum_{i < j} K_{ij}^{(G)} [(\cos(\theta_{0i} + \theta_i) - (\theta_{0j} + \theta_j) - 1)/2] \quad (38)$$

where

$$\theta_{0i} = \begin{cases} \pi; & i = 4, \\ 0; & i \neq 4. \end{cases} \quad (39)$$

Comparing Eq. (28) and (38), we get

$$\begin{aligned} J_{3,4} = J_{4,3} = K_{3,4}^{(G)}/4, \quad J_{4,5} = J_{5,4} = K_{4,5}^{(G)}/4, \\ J_{i,i+1} = J_{i+1,i} = -K_{i,i+1}^{(G)}/4, \quad \text{for } i \neq 3, 4 \end{aligned} \quad (40)$$

In addition to the difference between  $K_{i,i+1}^{(G)}$  and  $K_{i,i+1}^{(D)}$ , the lattice translational invariance is also broken in this expansion. However for high  $t_b$ , the difference between two methods becomes very small and the breaking of lattice translational invariance also becomes very small.

We also studied the expansion near other excited states, the conclusion is similar. Therefore we show that the effective Hamiltonian is given by Eq. (11) with continuous order parameter  $\sigma$  defined by Eq. (12).

## D. Gauss approximation for a real random temperature

The periodicity in the above discussion is not essential. We apply this method to real random temperature cases. The couplings obtained by two methods agree with well for weak couplings.

We show a typical example in Fig. 2. The ground state saddle point solution is shown in Fig. (2a). There are 18 blocks. After solving the Eq. (17) with the saddle point solution shown in Fig. (2a), we get the eigenvalues and the eigenfunctions. We divided the systems into 18 blocks and defined functions similar to Eq. (23). Then we expand the Hamiltonian of the  $\phi_y$  fluctuation and get the couplings  $K_{ij}^{(G)}$ . The comparison between the 18 couplings obtained by the two methods are given Fig. (2b).

The couplings obtained by two methods agree well in the range from  $10^{-4}$  to 1. The agreement is not good for  $K_{5,6}, K_{6,7}, K_{7,8}$  and  $K_{16,17}$  because the saddle point solution is not small in the regions between these couples of blocks.

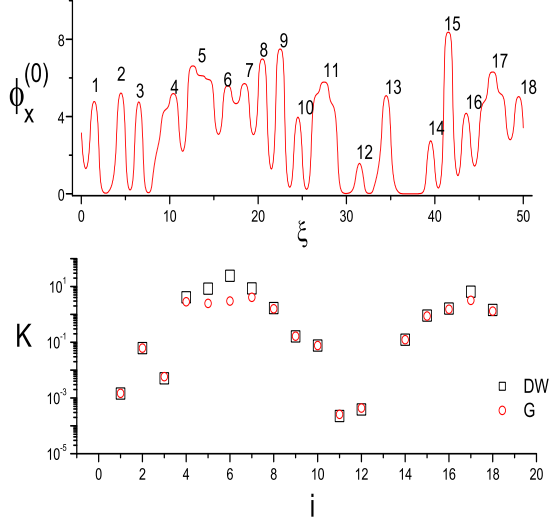


FIG. 3: (Color on line) (a) The ground state solution for certain random temperature realization. (b) The couplings between the adjoined blocks obtained by two methods. The black squares represent  $K_{i,i+1}^{(D)}$  and the red circles represent  $K_{i,i+1}^{(G)}$ .

#### IV. TWO DIMENSIONAL CASES

We consider the well lattice which is defined by

$$t(\xi, \eta) = \begin{cases} t_i; & 2l-1 < \xi \leq 2l \\ & 2m-1 < \eta \leq 2m \\ t_b; & \text{other cases.} \end{cases} \quad (41)$$

where  $l, m = 1, 2, 3$  and  $i = (m-1)*3 + l$ . The subscript of  $t_i$  is the label of the well, i.e., for convenience, we label the 9 wells with  $i = 1, 2, \dots, 9$  as shown in Fig. 4(a).

Assume the solution along x-direction, the saddle point equation is given by

$$-\frac{\partial^2 \phi_x}{\partial \xi^2} + \frac{\partial^2 \phi_x}{\partial \eta^2} + t(\xi, \eta) \phi_x + \phi_x^3 = 0. \quad (42)$$

where the usual periodic condition is used.

Expanding the Hamiltonian about this saddle point solution, the eigenmodes of  $\tilde{\phi}_y$  satisfy

$$-\frac{\partial^2 \varphi_n}{\partial \xi^2} + \frac{\partial^2 \varphi_n}{\partial \eta^2} + [t + (\phi_x^{(0)})^2] \varphi_n = \lambda_n \varphi_n \quad (43)$$

where  $\lambda_n$  is eigenvalues and  $\varphi_n$  are the eigenfunctions. Through the similar method given in section II, we obtain the couplings in Gauss approximation.

We first consider the simple case with uniform  $t_i = t_w = -30.0$  for  $i = 1, 2, 3, \dots, 9$ . The ground state solution for this well lattice is shown in Fig. (4b). It can

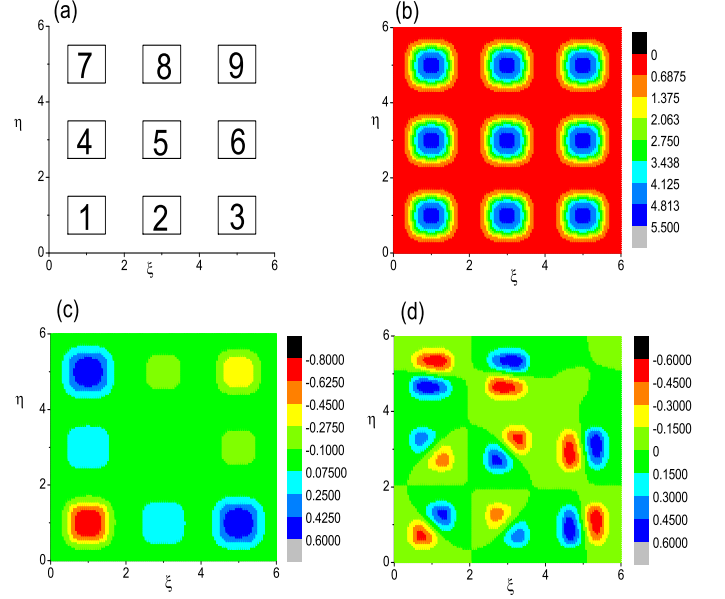


FIG. 4: (Color on line) (a) Well lattice. (b) The ground state solution. (c) The eigenfunction  $\varphi_6$ . (d) The eigenfunction  $\varphi_{16}$ . The temperatures are  $t_b = 30.0, t_w = -30.0$  for (b,c,d).

be seen that there are 9 blocks, which are the 9 cells of the well lattice. Using DW method, we can get the couplings between these blocks. Due to the lattice translational invariance, we can use  $K_{12}$  and  $K_{15}$  represent the coupling between nearest neighbors and next nearest neighbors respectively.

$t_b$	$K_{1,2}^{(D)}/4$	$-J_{1,2}$	$K_{1,5}^{(D)}/2$	$-J_{1,5}$	$R_\phi$	$R_\lambda$
40.0	0.035649	0.035720	0.000234	0.000199	187	491
30.0	0.086821	0.087172	0.00104	0.000847	96.5	203
20.0	0.24358	0.24549	0.00591	0.00455	34.6	72.3
10.0	0.84624	0.85015	0.0461	0.0336	11.2	19.9
0.0	3.6426	3.2314	0.348	0.253	3.28	4.75

Table 3: Couplings  $K^{(D)}$  by DW method and  $J_{ij}$  by Gauss approximation at different  $t_b$  and  $t_w = -30.0$ .

As shown in Fig. (4c), for the eigenfunction  $\varphi_6$ , the phase variations in the wells are much smaller than in the barriers. The first 9 eigenfunctions have this feature and other eigenfunctions do not have. As a example, we show  $\varphi_{16}$  in Fig. (4d). And for  $t_b > 0$ , the first 9 eigenvalues are much smaller than other eigenvalues. Therefore we take the first 9 eigenmodes into account and obtain the couplings between the clocks as we do in the preceding sections. The comparison between DW method and Gauss approximation are given in Table 3 for different  $t_b$ . The data in Fig. (3b, 3c, 3d) are for  $t_b = 30.0$ .

$t_b$	10.0		20.0		30.0	
$ij$	$K_{i,j}^{(D)}/4$	$-J_{i,j}^{(G)}$	$K_{i,j}^{(D)}/4$	$-J_{i,j}^{(G)}$	$K_{i,j}^{(D)}/4$	$-J_{i,j}^{(G)}$
12	0.6062	0.6384	0.1610	0.1651	0.0545	0.0552
23	0.8359	0.8466	0.2400	0.2429	0.0854	0.0859
31	1.1650	1.1270	0.3630	0.3617	0.1358	0.1359
45	0.6208	0.6649	0.1651	0.1711	0.0557	0.0566
56	0.7767	0.8107	0.2189	0.2246	0.0766	0.0776
64	1.5560	1.4610	0.5194	0.5114	0.2031	0.2022
78	0.8220	0.8111	0.2343	0.2345	0.0831	0.0832
89	0.3816	0.4314	0.0899	0.0955	0.0278	0.0286
97	0.4866	0.5384	0.1217	0.1286	0.0390	0.0401
14	1.0230	1.0130	0.3087	0.3099	0.1132	0.1135
47	0.3634	0.4064	0.0861	0.0903	0.0269	0.0264
71	1.7770	1.6400	0.6113	0.5977	0.2440	0.2421
25	1.1410	1.1080	0.3522	0.3509	0.1312	0.1311
58	0.4452	0.4790	0.1091	0.1136	0.0353	0.0359
82	0.6657	0.7261	0.1794	0.1886	0.0604	0.0619
36	0.9424	0.9379	0.2778	0.2792	0.1005	0.1009
69	0.5280	0.5488	0.1358	0.1384	0.0450	0.0454
93	0.6061	0.6679	0.1591	0.1679	0.0527	0.0541

Table 4: Couplings  $K_{ij}^{(D)}$  by DW method and  $J_{ij}^{(G)}$  by Gauss approximation with nonuniform  $t_i$  at different  $t_b$ .

In fact only the inhomogeneity rather than the periodicity of the temperature is essential. We also consider the random temperature cases with  $t_1, t_2, \dots, t_9$  being  $-30, -20, -50, -40, -17, -60, -35, -25, -15$  respectively. There are 18 couples of nearest neighbored blocks. In the table 4, we present the couplings between nearest neighbored couples at  $t_b = 30.0, 20.0, 10.0$ . As we can see that for  $t_b = 30.0$  the differences between the couplings obtained by two methods are much smaller than those at  $t_b = 10.0$ .

## V. SUMMARY

The continuous fluctuation about the saddle point solution is studied for XY-type Ginzburg-Landau Hamilto-

nian with random temperature. The final conclusion is that

(1) The effective Hamiltonian of blocks is a XY model.

(2) The DW method provides the excited states with block's phase being only  $0, \pi$ , and the Gauss approximation can describe the continuous phase fluctuation near the saddle point solutions.

(3) The couplings obtained by these two methods agree with each other well for the weak coupling cases.

DW method has a great advantage comparing with the Gauss approximation. For DW method, the size of the grid in the numerical calculation can be as large as  $2000 \times 2000$ , while in the Gauss approximation, the size of grid can only be as large as  $120 \times 120$  and the computing time is very long because of diagonalizing matrix. Therefore using DW method, the couplings between blocks can be conveniently calculated and the statistical properties of the couplings can be studied.

Our conclusion is consistent with the recent experiments and theoretical studies. Appearance of granular structures self-organized in homogeneously-disordered SC is discovered by the experiment [14] and shown by theoretical studies near the quantum critical point [15, 16].

Recently the excited state solutions of Bogliubov-de Gennes equations are solved for two dimensional negative-U Hubbard Hamiltonian with on-site disorder [17]. The excited states show that the system is self-organized into blocks. DW method is used to obtain the couplings between blocks. The authors claimed that the effective Hamiltonian between these blocks should be XY-type. The argument in this paper can be regarded as its corroborative evidence.

The author would like thank R. Ikeda for useful discussions, and K. Noda for his help in computing. This work is supported by the Scientific Research Foundation of State Education Ministry and the National Basic Research Program of China (Grant No. 2007CB925004).

- 
- [1] O. Plantevin, H. R. Glyde, B. Fåk, J. Bossy, F. Albergamo, N. Mulders and H. Schober, Phys. Rev. B **65**, 224505 (2002).
  - [2] K. Shirahama, Journal of Low Temperature Physics, **146**, 485 (2007).
  - [3] L. Merchant, J. Ostrick, R. P. Barber, Jr., and R. C. Dynes, Phys. Rev. B, **63**, 134508 (2001).
  - [4] M. Mondal, A. Kamlapure, M. Chand, G. Saraswat, S. Kumar, J. Jesudasan, L. Benfatto, V. Tripathi, and P. Raychaudhuri, Phys. Rev. Lett., **106**, 047001 (2011).
  - [5] K. K. Gomes, A. N. Pasupathy, A. Pushp, S. Ono, Y. Ando and A. Yazdani, Nature, **447**, 569 (2007).
  - [6] Z. Sun, J. F. Douglas, A. V. Fedorov, Y.-D. Chuang, H. Zheng, J. F. Mitchell and D. S. Dessau, Nature Physics **3**, 248 (2007).
  - [7] R. M. Eremina, I. V. Yatsyk, Ya. M. Mukovskii, H.-A. Krug von Nidda, and A. Loidl, JETP Letters, **85**, 51 (2007).
  - [8] X. T. Wu and K. Yamada, J. Phys. A: Math. & Gen. **37**, 3363 (2004).
  - [9] X. T. Wu, Phys. Rev. B **79**, 184208 (2009).
  - [10] X. T. Wu, Phys. Rev. E **82**, 010101(R) (2010)

- [11] V. Dotsenko, A. B. Harries, D. Sherrington, and R. B. Stincombe, *J. Phys. A: Math. & Gen.* **28** (1995) 3093.
- [12] S. E. Koonin, 1986 *Computational Physics* (New York: Benjamin/Cummings).
- [13] D. Bormann and H Beck, *Journal of Statistical Physics*, **76** (1994) 361.
- [14] D. Kowal and Z. Ovadyahu, *Solid State Commun.* **90**, 783 (1994).
- [15] A. Ghosal, M. Randeria, and N. Trivedi, *Phys. Rev. Lett.* **81**, 3940 (1998). *Phys. Rev. B*, **65**, 014501 (2001).
- [16] Yonatan Dubi, Yigal Meir and Yshai Avishai, *Nature* **449**, 876 (2007).
- [17] X. T. Wu and R. Ikeda. *Phys. Rev. B* **83**, 104517 (2011).